Applicability of a non-relativistic asymptotic description of high energy photoionization.

N. B. Avdonina[1], E. G. Drukarev[2] and R. H. Pratt[1]

[1]Department of Physics and Astronomy, University of Pittsburgh, Pittsburgh PA 15260, USA.
[2]St. Petersburg Nuclear Physics Institute, Gatchina, St. Petersburg 188300, Russia.

Abstract.

We show that while high energy photoionization cross sections converge to their asymptotic forms only at relativistic energies, the leading deviation from the asymptotic energy dependence of non-relativistic photoionization cross sections at high energy is the same for all cross sections. This factor can be obtained explicitly, and only asymptotic forms are needed for the remainder at high non-relativistic energies. Since the factor is common, ratios of photoionization cross sections reach their asymptotic values at much lower energies than the cross sections themselves. Results are presented both in independent particle approximation as well as including correlation effects, which modify the asymptotic behavior, especially for light elements or outer shells.

DOI: 32.80. Fb

I. Introduction.

In this paper we investigate the high-energy behaviour of cross sections for single photoionization of atomic systems. We find that a non-relativistic asymptotic approach is not in itself adequate for calculation of high energy photoionization cross sections, which converge to their asymptotic forms only at relativistic energies ω. However, in contrast to cross sections, the ratios of cross sections reach their asymptotic forms, except for the lightest elements, such as hydrogen and helium, at much lower energies. This is because a common explicit Coulombic-like factor (Stobbe factor) characterizes the leading deviations from asymptotic non-relativistic energy dependence of all photoionization cross sections at high energies. This fact allows us to explain recent experimental measurements [1,2] of photoionization cross section ratios utilizing asymptotic non-relativistic results. Utilizing these asymptotic ratios together with the Stobbe factor, the cross sections may be predicted with good accuracy. In our discussion of this behaviour we may go beyond independent particle approximation (IPA) and also include the consequences of electron - electron correlations, which modifies the asymptotic behavior of the ratios.

There had been a general belief [3] that for large ω photoionization can be described within the framework of independent particle approximation (IPA). However recent experiments of Dias et al. for the L shell of neon [1] and the M shell of argon [2] gave results in disagreement with IPA predictions. Examining the results it was found that correlation effects persist for transitions from subshells with orbital quantum numbers $\ell = 1$. These results were obtained in considering the asymptotic non-relativistic behaviour of the cross sections [4-6]. It may, however, be objected that the non-relativistic asymptotic behaviour is in fact not reached in the non-relativistic regime, so that it is irrelevant and only of academic interest (although see contrary arguments in [6]). Indeed, comparing results [7] obtained in the independent particle approximation (IPA) with the corresponding non-relativistic asymptotic predictions, we confirm that for the energies of the experiments (and well beyond) these cross sections are far from asymptotic. But in this paper we wish to point out that, in fact, the slowly convergent behaviour can be identified and explicitly factored out. The remaining high energy behaviour indeed reaches an asymptotic form in the non-relativistic regime (which will afterwards change, at relativistic energies).

We begin in Section II by reviewing the results for the asymptotic behaviour of non-relativistic high-energy photoionization cross sections. We also note the slow convergence of photoionization cross sections to their asymptotic forms. In Section III we analyze at the IPA level the approach to asymptotic behaviour. The leading correction to the asymptotic amplitude, which is exponentiated, is of the order $\pi Z/p$ [8] (we use atomic units, Z is the nuclear charge and p is the momentum of the photo-electron). This Stobbe factor [9], common for all subshells, cancels in the ratio of photoionization cross sections, explaining why ratios converge to asymptotic behaviour much faster then the cross sections themselves. In Section IV we go beyond independent particle approximation, confirming that correlations change the asymptotic behavior of all cross sections with non-zero angular momentum quantum number ℓ. However, we show that the leading correction to the asymptotic behaviour of the cross sections is still determined by the Stobbe factor Eq. (7). Consequently the asymptotic ratio of our subshell photoionization cross sections calculated in the non-relativistic approximation is in good agreement with the experimental results [1,2].

II. Asymptotic behaviour of the photoionization cross section.

The non-relativistic dipole IPA photoionization amplitude $\Phi^{I}_{n\ell}$ for a state with quantum numbers ($n\ell m$) is

$$\Phi^{I}_{n\ell} = <\Psi_p|g(\vec{r})|\Psi_{n\ell}>, \qquad (1)$$

with single-particle wave functions (outgoing electron) Ψ_p and (initial bound electron) $\Psi_{n\ell}$. The index I denotes the IPA case. The operator $g(\vec{r})$ describes the dipole electron-photon interaction. The amplitude $\Phi^{I}_{n\ell}$ depends on the form (length, velocity or acceleration) chosen for $g(\vec{r})$ if the wave functions Ψ_p and $\Psi_{n\ell}$ are approximate, not exact eigenfunctions. In this Section we consider the non-relativistic range of photon energies $c^2 > \omega >> I_{n\ell}$, where $I_{n\ell}$ is the photoionization energy (c=137 in the atomic units which we use in this paper).

Within the IPA framework each electron can be considered as moving in a common effective self-consistent field. Since near the origin this field has a nuclear point Coulombic behaviour, the asymptotic behaviour (i. e. the lowest order term in an expansion in powers of ω^{-1}) of the partial photoionization cross section is known to be [9]

$$\sigma^{I}_{n\ell}(\omega) = \alpha_{n\ell}\,\omega^{-(l+7/2)}\,[1+O(\omega^{-1/2})]\,, \qquad (2)$$

where the coefficient $\alpha_{n\ell}$ is independent of ω.

In IPA the photon interacts with and is directly absorbed by an atomic electron, which is ejected in a continuum state, while the other atomic electrons do not change their states. However, going beyond IPA, one can see another mechanism for photoionization. Instead of interacting with a $(n\ell)$ state, the photon can interact with a $(n'\ell')$ state, being absorbed and creating a hole in that state. Then the knocked-out electron can push an $(n\ell)$ electron into the $(n'\ell')$ hole by electron impact, again leaving an $(n\ell)$ hole and a continuum state. (Note that this second step takes place at distances of the order of the size of the Bohr $(n'\ell')$ orbit, rather than at the small distances at which the high energy photoabsorption process occurs.)

Recently it was realized [1,2] that, for $\ell = 1$, at high energies the second mechanism changes the behaviour of the photoionization cross section from that given by Eq. (2). This can be understood by considering the asymptotic behaviour of the amplitudes [5,6]. The full photoionization amplitude $\Phi_{n\ell}$ (beyond IPA) can be described as a sum of the amplitudes for the two mechanisms. In the first order random phase approximation with exchange (RPAE) [3] for the Coulomb interaction between atomic electrons, $V(r) = 1/|\vec{r}_1 - \vec{r}_2|$, the full amplitude $\Phi_{n\ell}$ is

$$\Phi_{n\ell} = \Phi^{I}_{n\ell} + \sum_{k,j} \frac{(\langle p,j\,|\,V\,|\,k,i\rangle - \langle p,j\,|\,V\,|\,i,k\rangle)\langle k\,|\,g(\vec{r})\,|\,j\rangle}{E_k - E_j - \omega + i\delta}\,, \qquad (3)$$

with summation over all intermediate single particle states k and over bound states j with quantum numbers $(n'\ell'm')$, with i the single particle bound state with quantum numbers $(n\ell m)$ which is photoionized. If k belongs to the continuum the summation should be replaced by integration (the infinitesimal parameter δ shifts the singularity into the complex plane and in this way defines the contour of integration). The second term of this equation gives the IPA breaking contribution to the amplitude. We suppress here all many-electron indices in the full many-electron wave functions except for those which involve the active electrons.

In the high energy limit the denominator in Eq. (3) is small only for high energy intermediate k-states for which momentum $\vec{k} \approx \vec{p}$ $\left(|\,\vec{p}\,| = \sqrt{2\omega - (Z/n)^2}\right)$. This means that the exchange matrix elements $\langle p,j\,|V|\,i,k\rangle$ are at least of order 1/p smaller than the direct matrix element $\langle p,j\,|V|\,k,i\rangle$ [10]. The denominator associated with the leading electron-electron Coulombic matrix element $\langle p,j\,|V|\,k,i\rangle$ contributes a factor 1/p to the asymptotic behaviour of the second term of Eq. (3) for any intermediate state [5,6]. Since the IPA matrix element factor $\langle j\,|\,g(\vec{r})\,|\,k\rangle \sim p^{-(7/2+\ell)}$ [Eq. (2)], which is $\sim p^{-7/2}$ whenever j is an s state, the second term in Eq. (3) has $p^{-9/2}$ asymptotic behaviour for any atom with at least a partially filled s-subshell in the initial state. Thus while for $\ell = 0$ the IPA asymptotic result (2) is correct, for $\ell > 0$ Eq. (2) should be changed to [5,6]

$$\sigma_{n\ell}(\omega) = \beta_{n\ell}\, \omega^{-9/2}\, [1+O(\omega^{-1/2})]. \tag{4}$$

Note that for $\ell = 1$ the functional dependence is not changed, but the value of the coefficient is modified: the IPA breaking effects result in the difference ($\beta_{n\ell}$-$\alpha_{n\ell}$) between the coefficients of Eqs. (2) and (4). For $\ell > 1$ the functional dependence on ω is altered. The ratios of cross sections of angular momenta $\ell > 0$ are independent of ω, unlike for the IPA result Eq. (3). The ratio $R_{s\ell} = [\sigma_{ns}(\omega)/\sigma_{n\ell}(\omega)] \sim \omega$, as in the IPA case, but the coefficient of ω is different. This explains the results presented in [1], where the slopes of the curves calculated in IPA and RPAE are different.

The first corrections to the asymptotic behaviours of the matrix elements (1) and (3) are smaller than the leading terms by only factors of order π/p. This implies a slow convergence of the cross sections to their asymptotic values. In Fig. 1 we show (dashed-dotted lines) results for the cross sections for neon obtained in the relativistic IPA approximation [7], multiplied by the factor $\omega^{7/2}$ for photoionization of the 2s subshell and by the factor $\omega^{9/2}$ for photoionization of the 2p subshell. Note that for low Z elements relativistic and retardation effects are small at low energies, so that one might have expected an initially flat behaviour of the curves, corresponding to Eqs. (2) and (4). In both cases, however, we see that this does not occur. The actual energy dependence is due to the slow convergence of cross sections to their non-relativistic asymptotic forms at lower energies and due to relativistic and retardation effects at higher energies; no regime exhibits non-relativistic asymptotic behaviour.

In the next Section we discuss this slow convergence of the IPA photoionization cross sections to their asymptotic behaviour at high photon energies, obtaining explicit expressions for the slowly convergent factors. We also show that the ratios of cross sections reach their asymptotic values at much lower energies then the cross sections. In the final Section we extend this discussion to the non-IPA case, when correlations are included.

III. The Stobbe factor

We use the result of the analytic screening theory [11,12] that in the limit of high energies IPA photoionization is determined at small distances, i. e. by the Coulombic behaviour of the wave functions near the nucleus. In the asymptotic non-relativistic case screening enters only in the change in the normalization N_i^I of the bound state wave function.

$$\sigma^I_{n\ell}(\omega) \sim \left(N_i^I\right)^2 / \left(N_i^C\right)^2 \sigma^C_{n\ell}(\omega), \tag{5}$$

where N_i^C is the normalization of the bound state of the hydrogenlike atom. The screening corrections due to wave function shapes (and normalization of the continuum wave function shapes) are, however, important at lower ω.

For the point-Coulomb case the full non-relativistic dipole photoionization cross sections $\sigma^{C}_{n\ell}(\omega)$ were initially obtained for the K-, L-shells [9] and then for the M-, N-shells [13]. In general they can be written in the form

$$\sigma^{C}_{n\ell}(\omega) = \text{const}\ N^2(\xi) P_{n\ell}(\xi^2/n^2)\ \exp[-2\pi\xi+4\xi\arctan(\xi/n)]\omega^{-(7/2+l)}, \tag{6}$$

where $\xi = Z/p$ and $N(\xi)$ is the normalization of the Coulombic continuum wave function, i.e. $N^2(\xi) = |\Gamma(1-i\xi)|^2 e^{\pi\xi}$. The polynomial ratio $P_{n\ell}(\xi^2/n^2)$ depends weakly (through the coefficients of the powers of ξ) on the orbital quantum number ℓ of the initial state.

Note that the slow convergence of the cross sections to the exact asymptotic result Eq. (2) is primarily due to the product of $\exp(\pi\xi)$ and $\exp[-2\pi\xi+4\xi\arctan(\xi/n)] \to \exp(-\pi\xi)$ for small $\xi = Z/p$, where $\exp(\pi\xi)$ comes from the continuum state normalization factor $N^2(\xi)$. All other factors in Eq. (6) have faster convergence, $O(\xi^2)$. This leading term in the departure of the Coulombic cross section $\sigma^{C}_{n\ell}(\omega)$ from its asymptotic value,

$$S(\xi)= \exp(-\pi\xi), \tag{7}$$

we will call the Stobbe factor, recognizing the original Coulombic calculation of Stobbe [9] in which it was obtained; it is independent of n, ℓ. Thus the leading correction to the asymptotic behaviour of the cross sections $\sigma^{I}_{n\ell}(\omega)$ is determined by a factor of order $\pi\xi$ which is common for all transitions from all atomic subshells.

In Fig. 1 we show the scaled cross sections $\omega^{7/2}\sigma^{I}_{2s}(\omega)/S(\xi)$ and $\omega^{9/2}\sigma^{I}_{2p}(\omega)/S(\xi)$ for Ne, which reach their asymptotic behaviour at high, but still non-relativistic, energies (above 10 keV). However the remaining energy dependence $O(\xi^2)$ is still important at most non-relativistic energies. The cancellation of the Stobbe factor $S(\xi)$ in ratios leads to a faster convergence of the ratios of the photoionization cross sections to their asymptotic form. We see in Fig. 1 that the ratio of these cross sections in fact converges much more rapidly (divided by ω to remove the asymptotic energy dependence, it is flat already below 10 keV), indicating additional cancellation of common factors.

The Stobbe factor $S(\xi)$ determines the behaviour of cross sections only at very high energies $p \gg \pi Z$ ($\pi\xi \ll 1$). For lower energies, larger n, or for heavier atoms the terms of order ξ^2 play an important role in the behaviour of the photoionization cross section $\sigma^{I}_{n\ell}(\omega)$. The pre-asymptotic energy dependence of the cross section $\sigma^{I}_{n\ell}(\omega)$ is primarily determined by the generalized Stobbe factor

$$S_n(\xi) = |\Gamma(1-i\xi)|^2 \exp[-\pi\xi+4\xi\arctan(\xi/n)] \tag{8}$$

of Eq. (6), which includes the normalization factor $N(\xi)$, i.e. one is still neglecting the energy dependence in the polynomial $P_{n\ell}(\xi^2/n^2)$ and that due to screening. The factor $|\Gamma(1-i\xi)|^2 = 2\pi\xi/(e^{\pi\xi}-e^{-\pi\xi})$ differs from one by terms of order $\pi^2\xi^2/6$; these start being important already for $p \leq \pi Z/\sqrt{6}$ ($\pi^2\xi^2/6 \geq 1$). The arctangent term $4\xi\arctan(\xi/n)$ in the exponential is of order $4\xi^2/n$, and for small n < 3 it can play an even more important role than the corrections in $|\Gamma(1-i\xi)|^2$. Note that $S_n(\xi)$ is common for all transitions from the same atomic shell, since it does not depend on ℓ. Divided by this factor, $\omega^{7/2}\sigma^I_{2s}(\omega)$ and $\omega^{9/2}\sigma^I_{2p}(\omega)$ converge to their asymptotic forms much faster than the cross sections themselves or the cross sections when only divided by $S(\xi)$ of Eq. 7 (Fig. 2a).

The remaining second order corrections are smaller in their effect than those which are included in the expression for $S_n(\xi)$ (Eq. 8). For light atoms (or inner shells of heavier atoms), these remaining effects are important only at energies lower than a few keV (but note, this is the region of energies for which experiments are now available). These remaining corrections are of two types. First of all, there are the polynomial ratios $P_{nl}(\xi^2/n^2)$ in the Coulombic cross section (5). Being of order ξ^2/n^2 their influence on the cross sections is less than the effect of $\exp[4\xi\arctan(\xi/n)]$ and the corrections in $|\Gamma(1-i\xi)|^2$ in Eq. (8). In Fig. 2b we show that the influence of the polynomial ratio $P_{2s}(\xi^2/2^2) = 1+3(\xi/2)^2/[1+(\xi/2)^2]$ for 2s and $P_{2p}(\xi^2/2^2) = 1+8(\xi/2)^2/3[1+(\xi/2)^2]$ for 2p on the cross sections in Ne is weaker and only affects convergence below a few keV.

When screening in the potential at small distances r is characterised by an expansion in powers of r, the remaining second order corrections will be characterised by the coefficients of this expansion which depend on the screening. Accordingly [11,12] screening contributes to the photoionization cross section through the normalization of the initial bound and continuum state wave functions, as well as in corrections to the reduced matrix element which vanish asymptotically. One part of these screening corrections, already present asymptotically, comes from the screening effects on the bound state normalization factor $(N^I_i)^2$ in Eq. (5). One can show that the screening effect due to the change in the normalization of the initial bound and continuum state wave functions can largely be taken into account by shifting the Coulombic ξ values in N^I_i to their physical values $\xi_{n\ell} = Z/\sqrt{2(\omega - I_{n\ell})}$, with $I_{n\ell}$ the physical ionization energy. This means that for given photon energy we should write the continuum normalization in terms of $\xi_{n\ell}$ as $N^2_n(\xi_{n\ell}) = |\Gamma(1-i\xi_{n\ell})|^2 e^{\pi\xi_{n\ell}}/(2\pi)^3$. Division of the cross sections $\omega^{7/2}\sigma^I_{2s}(\omega)$ and $\omega^{9/2}\sigma^I_{2p}(\omega)$ of Ne by such an adjusted generalized Stobbe factor

$$S_{n\ell}(\xi_{n\ell}) = P_{n\ell}(\xi)|\Gamma(1-i\xi_{n\ell})|^2 \exp[-\pi(2\xi-\xi_{n\ell})+4\xi\arctan(\xi/n)], \qquad (9)$$

(which includes also the polynomial ratios coming from the Coulombic cross section of Eq. (6)) makes them flatter even at low energies. In Fig. 2b we show this for the cross sections for neon obtained in the relativistic IPA approximation [7]. Note also that the ratio $\sigma^I_{2s}(\omega)/\omega\sigma^I_{2p}(\omega)$ is approximately flat already by an energy of about a few keV.

In Fig. 3a the results of division by the generalized Stobbe factors $S_n(\xi)$ of Eq. (8) and adjusted generalized Stobbe factors $S_{n\ell}(\xi_{n\ell})$ of Eq. (9) are shown for the 2s and 2p photoionization cross sections of Ne calculated in the single particle non-relativistic Hartree-Fock approximation for energies lower than 1 keV. We can see that $\omega^{(7/2}\sigma^I_{2s}(\omega)$ and $\omega^{(9/2}\sigma^I_{2p}(\omega)$ devided by the Stobbe factors are only approximately flat at $\omega = 700$ eV, because of further screening effects which are not yet taken into account, but are important for outer subshells at low energies.

We see similar behaviour in the case of photoionization from Ar, where photoionization from 3s and 3p subshells was measured [2]. With increasing Z the cancellation effect of the common energy dependent factors in the ratio of the cross sections manifests itself at higher energies. Since Ar is a much heavier atom than Ne, its asymptotic behaviour begins at much higher energies, where non-relativistic considerations are not valid. Our calculations, however, show that the IPA ratios $\sigma^I_{2s}(\omega)/\omega\sigma^I_{2p}$ and $\sigma^I_{3s}(\omega)/\omega\sigma^I_{3p}$ are still approximately flat at the non-relativistic energies of the experiment (about 1 keV), in correspondence with Eq. (2) (Fig.3b).

Thus we can conclude, that due to the common Stobbe factor $S_n(\xi)$ of Eq. (8) in cross sections for photoionization from subshells of given n with orbital quantum numbers ℓ' and ℓ, the IPA ratio of these cross sections converges rapidly to the asymptotic value $R_{\ell\ell'} \sim \omega^{\ell-\ell'}$. For different shells the ratio $\sigma^I_{n'\ell'}(\omega)/\sigma^I_{n\ell}(\omega)$ also converges to asymptotic values faster than the cross sections [due to the common Stobbe factor $S(\xi)$ from (7)], although in this case it can occur at energies so high that non-relativistic considerations are not valid.

In this Section we have demonstrated within IPA the applicability of asymptotic non-relativistic ratios of cross sections. However, as we saw in Section II, the independent particle approximation is not sufficient. Going beyond IPA, we have already considered the case of the Hartree-Fock approximation, finding similar behaviours for ratios of cross sections. In the next Section we will extend our demonstration of the fast convergence of ratios, showing that it remains valid even when correlations effects are included.

IV. Beyond IPA- correlation effects.

We will now discuss how electron correlations change the results. We begin by showing that at high photon energy the leading correlation contributions to the RPAE amplitude, given by the second term of Eq. (3), can be written as a linear combination of IPA terms, with coefficients of order p^{-1} in the photoelectron momentum.

To obtain these leading terms at high-energy we neglect the exchange matrix element $\langle p, j \,|\, V \,|\, i, k \rangle$ in Eq. (3) and write

$$\Phi_{n\ell} = \Phi^{I}_{n\ell} + \sum_{k,j} \frac{\langle p, j \,|\, V \,|\, k, i \rangle \langle k \,|\, g(\vec{r}) \,|\, j \rangle}{E_k - E_j - \omega + i\delta} \quad , \tag{10}$$

where j is the single particle bound state with quantum numbers (n'ℓ'm'), and i is the bound state with quantum numbers (nℓ m).

The main contribution to the sum over k comes from continuum states with high momenta $\vec{k}$. Since the final electron momentum $\vec{p}$ is also large the wave functions Ψ_k and Ψ_p in the electron-electron interaction matrix element (though usually not in the radiation interaction matrix element) can be approximated as plane waves, giving

$$\langle p, j \,|\, V \,|\, k, i \rangle = \frac{1}{(2\pi)^3 f^2} \int \Psi^{*}_{n'\ell'}(\vec{r}) e^{i\vec{f}\cdot\vec{r}} \Psi_{n\ell}(\vec{r}) d\vec{r} \quad . \tag{11}$$

Note that for a small momentum transfer $\vec{f} = \vec{p} - \vec{k}$ the only large matrix element in Eq. (10) is $\langle p, j \,|\, V \,|\, k, i \rangle$. Eq. (10) can be then rewritten as a linear combination of the IPA amplitudes $\Phi^{I}_{n'\ell'}$:

$$\Phi_{n\ell} = \Phi^{I}_{n\ell} + \sum_{n'\ell'} \Lambda_{n\ell, n'\ell'} \Phi^{I}_{n'\ell} \quad , \tag{12}$$

where n'ℓ' are the quantum numbers of the j-state. The coefficients $\Lambda_{n\ell, n'\ell'}$ can be expressed in terms of the matrix elements of simple operators

$$\Lambda_{n\ell, n'\ell'} = \frac{1}{(2\pi)^3} \int \left\langle nl \middle| e^{i\vec{f}\cdot\vec{r}} \middle| n'l' \right\rangle \frac{d^3 f}{f^2 [E_f - (\vec{p}\cdot\vec{f}) + i\delta]} . \tag{13}$$

For large p the coefficients are of order 1/p. An explicit expression for $\Lambda_{n\ell, n'\ell'}$ was obtained in [14]. Since for the transitions from s states the first IPA matrix element in Eq. (12), $\Phi^{I}_{n\ell} \sim p^{-7/2}$, and the second term has at least $p^{-9/2}$ asymptotic behaviour, for $\ell = 0$ the asymptotic result for the photoionization amplitude is the same as the IPA result of Eq. (2). For any atom with at least a partially filled s-subshell in the initial state, for transitions from states with $\ell > 0$, the asymptotic behaviour of the cross sections $\sigma_{n\ell}(\omega)$ are determined by the part of the second term of the amplitude (12) in which $\ell' = 0$. If only correlations with the s-state $\ell' = 0$ are significant $\sigma_{n\ell}(\omega) \sim \sigma^{I}_{ns}(\omega)/p$ and we get the asymptotic behaviour of Eq. (4).

For our purpose, however, what is important is that, according to Eq. (12), the asymptotic behaviour of the photoionization amplitude is determined by the common Stobbe factor S(ξ) of Eq. (7). Thus, as in the IPA case, these cross sections, which have the same common factor as for $\sigma^{I}_{n's}(\omega)$, are only slowly convergent to asymptotic values. In the case of $\ell = 1$ both terms in the amplitude (12) are of the same order, and both involve the same common Stobbe factor in their amplitudes. For $\ell = 0$ the IPA term is dominant, again with the same Stobbe factor.

Since correlations are bigger for electrons of the same shell we can assume that the interaction between the atomic electron and the ionized electron is not altered by the bound electrons of another shell, and in Eq. (12) can include only terms with n' = n. In Fig. 3a we present results for RPAE photoionization cross sections fron 2s and 2p subshells of Ne divided by the generalized Stobbe factor $S_n(\xi)$ of Eq. (8). This Stobbe factor, which includes terms of order ξ^2, and which plays an important role at lower p, will be the same for $\sigma_{n\ell}(\omega)$ and $\sigma^{I}_{n\ell}(\omega)$. In Fig. 3a we can see that RPAE results are quite different from the IPA cross sections. However, for photoionization from the 2s state the difference becomes smaller with increasing energy. This reflects the fact that the asymptotic leading term of $\sigma_{2s}(\omega)$ (Eq. (2)) is the same in both the RPAE and IPA cases. However, in the case of photoionization from the 2p state, the IPA breaking effect results in the difference $(\beta_{2p}-\alpha_{2p})$ between the coefficients of Eqs. (2) and (4), and therefore we do not see a decreasing difference between IPA and RPAE results.

Despite the slow convergence of the photoionization cross sections themselves, we can expect a fast convergence of their ratios, so that non-relativistic values of the ratios will be achieved within the non-relativistic range of photon energies. We demonstrate this in Fig. 3a for photoionization of Neon. Since $R_{sp}(\omega)=[\sigma_{2s}(\omega)/\sigma_{2p}(\omega)] \sim \omega$, as in the IPA case (but with a different coefficient of ω), the $R_{sp}(\omega)/\omega$ curve in Fig. 3a calculated in RPAE is approximately flat. The ratio follows the asymptotic law with an accuracy of better than 10% for photon energies exceeding 700 eV.

In Fig. 3b we present results for the ratios R_{sp} for n=2 $[R_{2sp}(\omega)/\omega]$ and n=3 $[R_{3sp}(\omega)/\omega]$ subshells of Ar, calculated in the Hartree-Fock and RPAE approximations. The ratios, which are divided by ω, are already close to constant (not the same constant) at energies of about 1 keV, but the cross sections themselves are far from asymptotic, as had been noted in [5,6]. Our RPAE calculations involve couplings between M and L shell electrons. It is known [3] that near the ionization threshold the correlations are much more important for the outer shells. We can see the same effect at high energies as well - our Hartree-Fock and RPAE $R_{2sp}(\omega)/\omega$ curves for n=2 in Fig. 3b are only slightly different, while correlations enhance the Hartree-Fock $R_{3sp}(\omega)/\omega$ in the transitions from 3p subshell by about 25%.

Correlations in outer shells at high energies are also important for positive ions. We show their effect for K^+ ions in Fig. 4. The difference between Hartree-Fock and RPAE $R_{2sp}(\omega)/\omega$ values is as big as for neutral Ar, i. e. about 25%.

V. Conclusions

In summary, we have shown that, despite the fact that high-energy photoionization cross sections do not converge to their non-relativistic asymptotic behavior (except maybe in the lightest elements, such as hydrogen and helium) in the non-relativistic photon energy region, a non-relativistic asymptotic approach is still applicable for calculation of their ratios. The reason is the cancellation of explicitly known common Coulombic-like Stobbe factors Eq. (7), which characterize the primary deviations from the asymptotic non-relativistic energy dependence. Utilizing the asymptotic ratios together with the Stobbe factor, the cross sections may be predicted with good accuracy. This supports our non-relativistic consideration of the asymptotic behaviour of the ratios of the photoionization cross sections in paper [6].

At lower energies we still can find a common factor, which now depends on the principal quantum number n, but is independent of the orbital quantum numbers (Eq. (8)). Cancellation still occurs for photoionization cross sections from the same atomic shell. This explains the behaviour of the ratios of the photoionization cross sections from s- and p-subshells in Ne and Ar [1,2]. Even at very low energies (below 1000 eV for the atoms we consider in this paper) cancellation of the generalized Stobbe factors (Eq. (9)) makes the ratios of the cross sections close to asymptotic.

Going beyond independent particle approximation, we confirm that correlations change the asymptotic behavior of all cross sections with non-zero angular momentum quantum number ℓ. However, we show that the leading correction to the asymptotic behaviour of the cross sections is still determined by the Stobbe factor. Consequently the asymptotic ratio of our subshell photoionization cross sections, calculated in the non-relativistic approximation with correlations, is in good agreement with the experimental results [1,2].

Here we have considered non-relativistic photoionization. The Stobbe factor can be also identified within a relativistic approach, but in this case it is independent of the total energy E, since now at high energy ξ = EZ/p does not depend on E ~ p. However, it is known that in the relativistic case there is also slow convergence with energy of the photoionization cross sections in the parameter 1/p.

Acknowledgments

We are very thankful to J. E. Burgdoerfer and Tihomir Suric for valuable discussions. This work was supported in part by the National Science Foundation under grant PHY 9601752.

References

[1] E. W. B. Dias et al, Phys. Rev. Lett. 78, 553 (1997).
[2] D. L. Hansen et al, Phys. Rev. A 60, R2641 (1999).
[3] M. Ya. Amusia, "Atomic Photoeffect" (Plenum Press, N. Y., 1990).
[4] H. A. Bethe and E. E. Salpeter, 1971 Quantum Mechanics of One- and Two-Electron Atoms, (Plenum/Rosetta, NY)
[5] E. G. Drukarev, Nina Avdonina, and R. H. Pratt, Bull. Am. Phys. Soc. 44, 132 (1999).

[6] M. Ya Amusia., N. B. Avdonina, E. G. Drukarev, S. T.Manson, and R. H. Pratt, Phys. Rev. Lett. 85, 4703 (2000).
[7] J. H. Scofield, UCRI, Report No. 51326 (1973) (unpublished).
[8] T. Suric, In Frontiers of Physics 1998 (edited by S. P. Chia and D. A. Bradley, World Scientific, Singapore), 125 (2000).
[9] M Stobbe., Ann. D. Phys. 7, 661, (1930).
[10] V. I. Ochkur and L. Burkova, Sov. Phys. JETP 49(1),38 (1979).
[11] R. H. Pratt and H. K. Tseng, Phys. Rev. A5, 1063 (1972).
[12] S. D. Oh, J. McEnnan, and R. H. Pratt, Phys. Rev. A14, 1428 (1976).
[13] J. Harriman, Phys. Rev. 101, 594 (1956).
[14] E. G. Drukarev and M. I. Strikman, Sov. Phys. JETP 64, 686 (1986).

Figures captions

Fig. 1. Cross sections for transitions from 2s (2s-curves) and 2p (2p-curves) subshells of Ne obtained in the relativistic IPA approximation [7] (in barn multiplied by powers of keV). Dashed-dotted lines are used for cross sections multiplied by the factor $\omega^{7/2}$ for photoionization of the 2s subshell, and by the factor $\omega^{9/2}$ for photoionization of the 2p subshell (ω in keV). Dashed lines are used for the cross sections $\omega^{7/2}\sigma^{I}_{2s}(\omega)$ and $\omega^{9/2}\sigma^{I}_{2p}(\omega)$ divided by the Stobbe factor $S(\xi)$ (2s/S- and 2p/S-curves) (Eq. (7)) (and divided by a factor of 10 for convenience in presentation). The ratio $\sigma^{I}_{2s}(\omega)/\omega\sigma^{I}_{2p}(\omega)$ (in keV^{-1} multiplied by 10^4) is shown with a solid line.

Fig. 2. (a) Cross sections $\omega^{7/2}\sigma^{I}_{2s}(\omega)$ and $\omega^{9/2}\sigma^{I}_{2p}(\omega)$ of Ne obtained as in Fig. 1, divided by $S(\xi)$ [dashed 2s/S- and 2p/S-lines, Eq. (7)], and by generalized factor $S_2(\xi)$ [dashed-triple-dotted 2s/S_2- and 2p/S_2-lines, Eq. (8)] .
(b) $\omega^{7/2}\sigma^{I}_{2s}(\omega)$ and $\omega^{9/2}\sigma^{I}_{2p}(\omega)$ (in barn multiplied by powers of keV) divided by the adjusted generalized Stobbe factor $S_{2\ell}(\xi_{2\ell})$ of Eq. (9) [thick dotted 2s/S_{2s} - and 2p/S_{2p} - lines] as well, as divided by $S_2(\xi)$ [dashed-triple-dotted 2s/S_2- and 2p/S_2-lines, Eq. (8)]. The cross divided by both $S_2(\xi)$ and the polynomial ratio $P_{2s}(\xi^2/2^2)$ are also shown with thin dotted s- and p-lines for comparison. The ratio $\sigma^{I}_{2s}(\omega)/\omega\sigma^{I}_{2p}(\omega)$ (ω) (in keV^{-1} and multiplied by 10^4) is shown with a solid line.

Fig. 3. (a) The cross sections for Ne in the Hartree-Fock approximation, divided by generalized factor $S_2(\xi)$ of Eq. (8) [dashed-triple-dotted 2s/S_2- and 2p/S_2-lines] and the adjusted generalized Stobbe factor $S_{2\ell}(\xi_{2\ell})$ of Eq. (9) (thick dotted s- and p-lines). The cross sections for Ne obtained in the same way but in RPAE are shown with long dashed s- and p-lines (in barn multiplied by powers of keV). The ratios $R_{sp}(\omega)/\omega$ (in keV^{-1}) are obtained in the Hartree-Fock approximation (solid lines) and in RPAE (dashed lines).
(b) The ratios $R_{2sp}(\omega)/\omega$ and $R_{3sp}(\omega)/\omega$ (in keV^{-1}).for Ar in the Hartree-Fock approximation (solid lines) and in RPAE (dashed lines).

Fig. 4. The cross sections $\omega^{7/2}\sigma^{I}_{3s}(\omega)$ and $\omega^{9/2}\sigma^{I}_{3p}(\omega)$ in RPAE (in barn multiplied by powers of keV) are shown with dashed-dotted lines), and the ratios $R_{3sp}(\omega)/\omega$ (in keV^{-1} and multiplied by 10^4) for K^+ in the Hartree-Fock approximation (solid lines) and in RPAE (dashed lines).

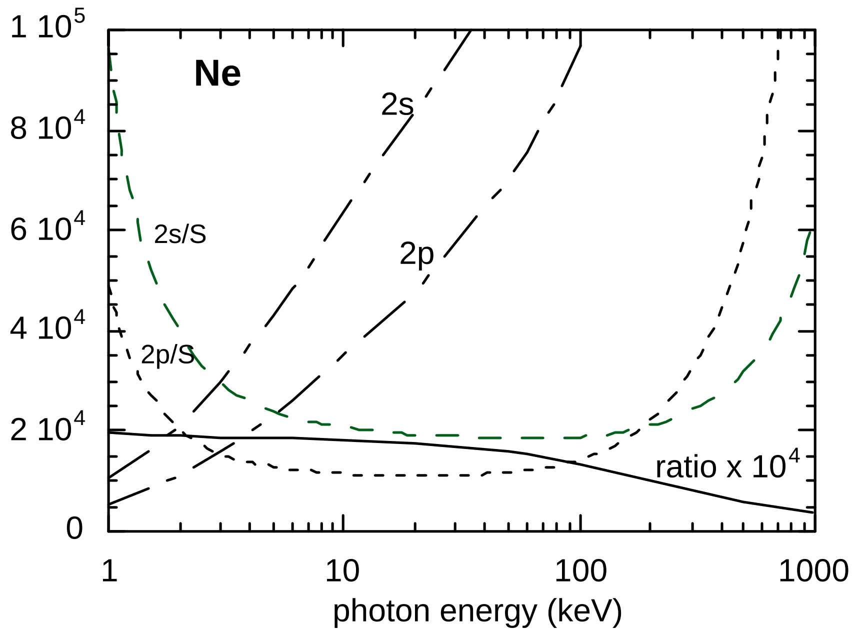

Ne
2s
2p
2s/S
2p/S
ratio x 10^4
1 10^5
8 10^4
6 10^4
4 10^4
2 10^4
0
1
10
100
1000
photon energy (keV)

Fig. 1.

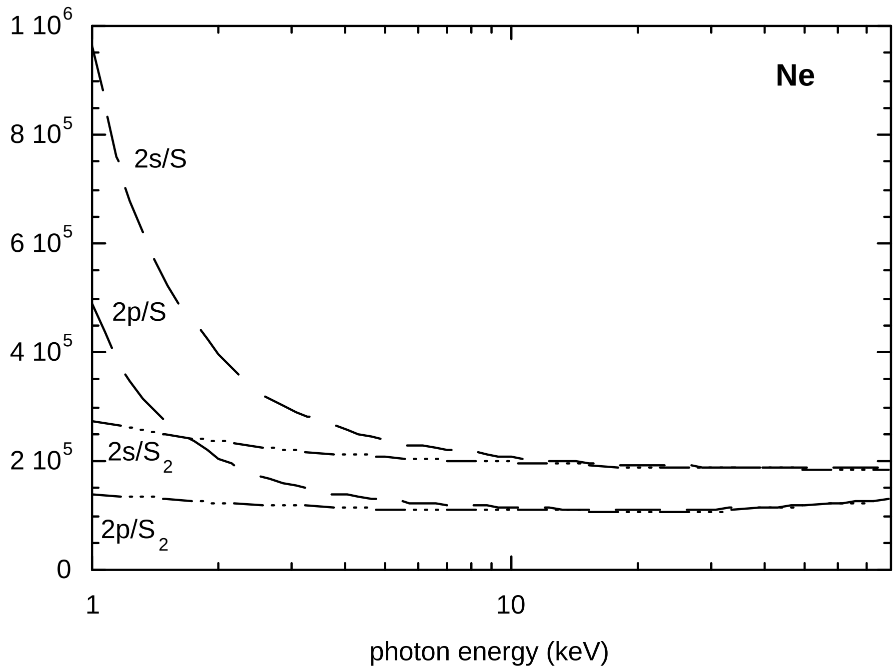
1 10^6
8 10^5
6 10^5
4 10^5
2 10^5
0
1
10
photon energy (keV)
Ne
2s/S
2p/S
2s/S_2
2p/S_2

Fig. 2a

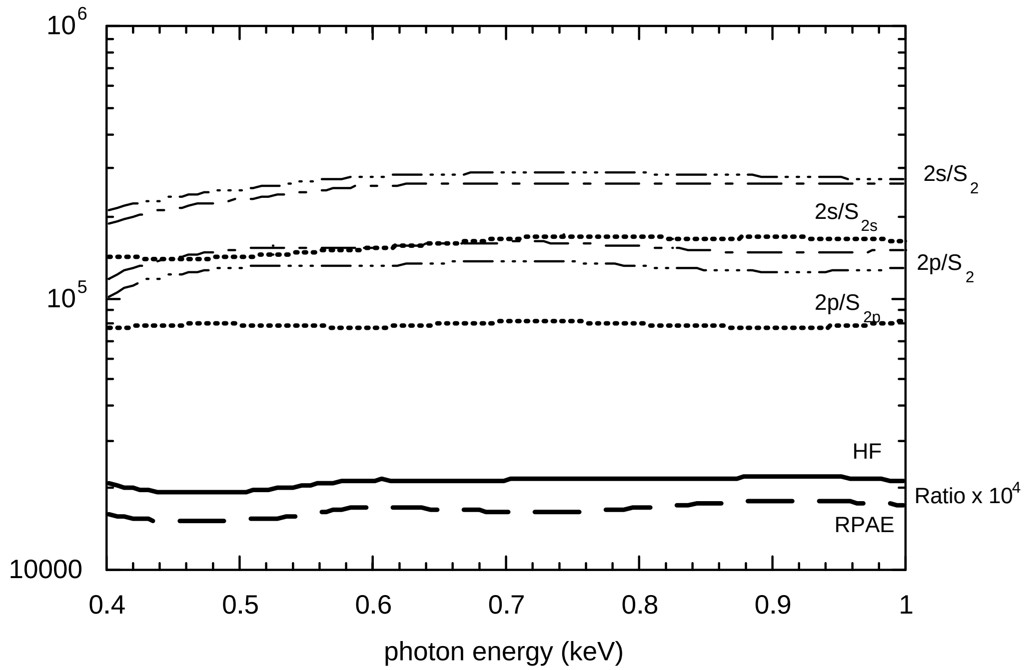

10^6
10^5
10000
0.4
0.5
0.6
0.7
0.8
0.9
1
photon energy (keV)
2s/S 2
2s/S 2s
2p/S 2
2p/S 2p
HF
Ratio x 10^4
RPAE

Fig. 2b

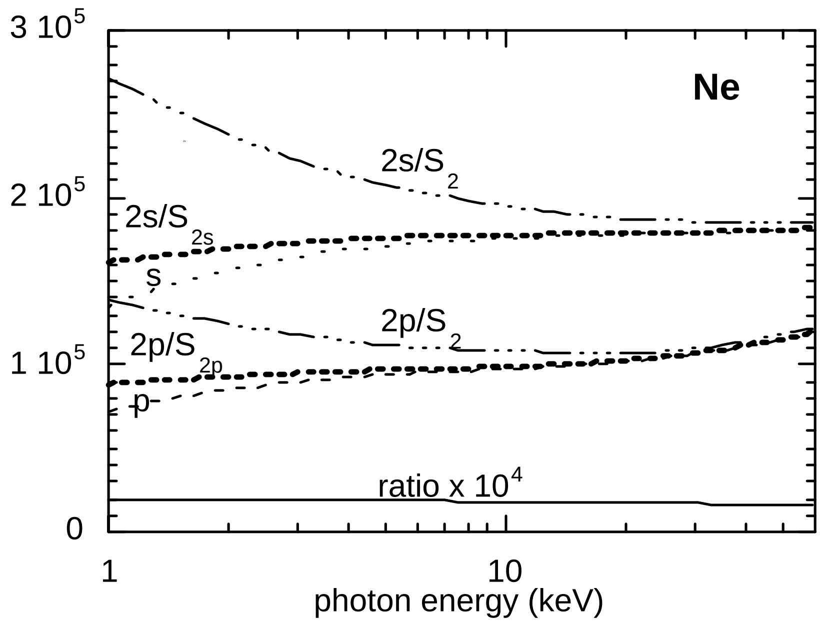
Ne
2s/S2
2s/S2s
s
2p/S2
2p/S2p
p
ratio x 10^4
3 10^5
2 10^5
1 10^5
0
1
10
photon energy (keV)

Fig. 3a

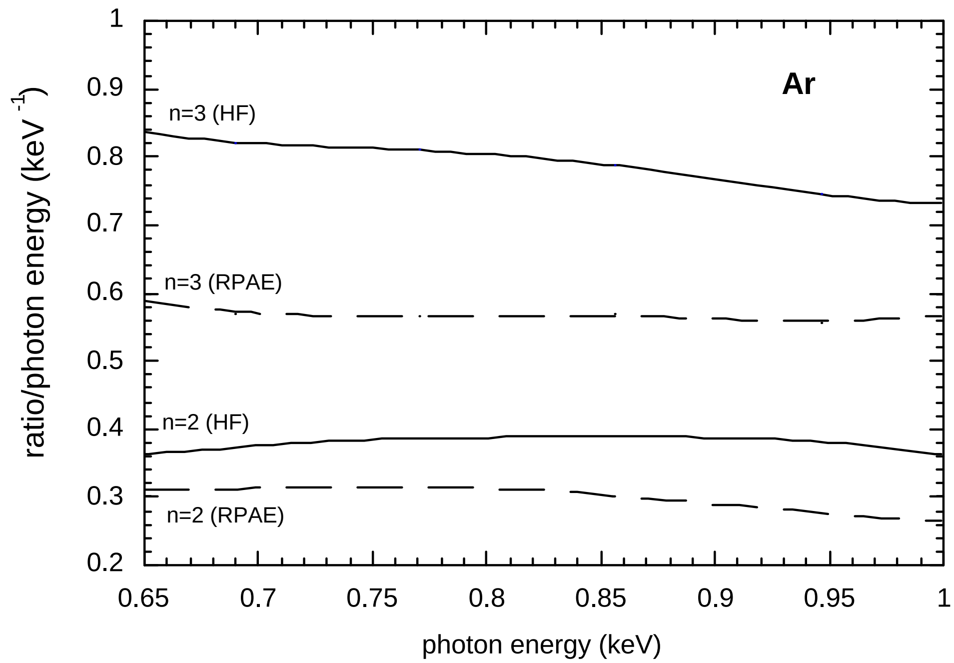
Ar
n=3 (HF)
n=3 (RPAE)
n=2 (HF)
n=2 (RPAE)
ratio/photon energy (keV $^{-1}$)
photon energy (keV)
1
0.9
0.8
0.7
0.6
0.5
0.4
0.3
0.2
0.65
0.7
0.75
0.8
0.85
0.9
0.95
1

Fig. 3b

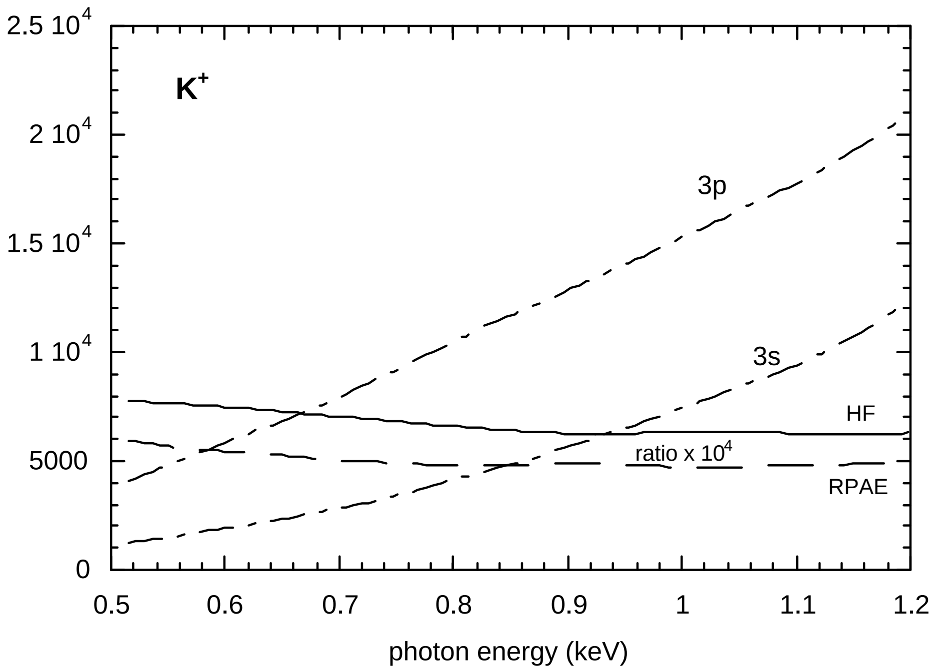
2.5 10^4
2 10^4
1.5 10^4
1 10^4
5000
0
K+
3p
3s
HF
ratio x 10^4
RPAE
0.5
0.6
0.7
0.8
0.9
1
1.1
1.2
photon energy (keV)

Fig. 4